Journal of General Virology (2009), **90**, 2956–2964 **DOI** 10.1099/vir.0.014282-0

Rat respiratory coronavirus infection: replication in airway and alveolar epithelial cells and the innate immune response

C. Joel Funk,[1] Rizwan Manzer,[1] Tanya A. Miura,[2] Steve D. Groshong,[1] Yoko Ito,[1] Emily A. Travanty,[1] Jennifer Leete,[1] Kathryn V. Holmes[3] and Robert J. Mason[1]

Correspondence
Robert J. Mason
masonb@njhealth.org

[1]National Jewish Health, 1400 Jackson Street, Denver, CO 80206, USA

[2]Department of Microbiology, Molecular Biology and Biochemistry, University of Idaho, Moscow, ID 83844, USA

[3]Department of Microbiology, University of Colorado Denver, Aurora, CO 80110, USA

The rat coronavirus sialodacryoadenitis virus (SDAV) causes respiratory infection and provides a system for investigating respiratory coronaviruses in a natural host. A viral suspension in the form of a microspray aerosol was delivered by intratracheal instillation into the distal lung of 6–8-week-old Fischer 344 rats. SDAV inoculation produced a 7 % body weight loss over a 5 day period that was followed by recovery over the next 7 days. SDAV caused focal lesions in the lung, which were most severe on day 4 post-inoculation (p.i.). Immunofluorescent staining showed that four cell types supported SDAV virus replication in the lower respiratory tract, namely Clara cells, ciliated cells in the bronchial airway and alveolar type I and type II cells in the lung parenchyma. In bronchial alveolar lavage fluid (BALF) a neutrophil influx increased the population of neutrophils to 45 % compared with 6 % of the cells in control samples on day 2 after mock inoculation. Virus infection induced an increase in surfactant protein SP-D levels in BALF of infected rats on days 4 and 8 p.i. that subsided by day 12. The concentrations of chemokines MCP-1, LIX and CINC-1 in BALF increased on day 4 p.i., but returned to control levels by day 8. Intratracheal instillation of rats with SDAV coronavirus caused an acute, self-limited infection that is a useful model for studying the early events of the innate immune response to respiratory coronavirus infections in lungs of the natural virus host.

Received 18 June 2009
Accepted 2 September 2009

INTRODUCTION

The large volume of air inhaled each day and the extensive surface area of the lung makes the respiratory system especially vulnerable to airborne infectious agents. These pathogens include many respiratory viruses such as influenza virus, respiratory syncytial virus, rhinovirus and coronaviruses (CoVs). Respiratory tract infections are the leading cause of infectious disease globally (WHO, 2004). The outbreak of severe acute respiratory syndrome (SARS) in 2002–2003 emphasized the vulnerability of humans to respiratory virus diseases and the potential for high morbidity and mortality in viral infections of the lower respiratory tract. The aetiological agent of SARS was identified as a coronavirus (SARS-CoV) derived from an animal reservoir (Fouchier *et al.*, 2003). Besides human infections, CoVs cause respiratory, enteric and neurological infections in a variety of birds and mammals (Weiss & Navas-Martin, 2005). Five human CoVs have been identified to date, all of which cause respiratory tract infections. Human CoVs 229E and OC43 were first identified in the 1960s, and they cause up to 15–35 % of the adult colds in otherwise healthy individuals (Kahn & McIntosh, 2005). After the discovery of SARS-CoV, two additional human CoVs were identified, NL63 and HKU1 (van der Hoek *et al.*, 2004; Woo *et al.*, 2005). On a global basis, the human CoVs 229E, OC43, HKU1 and NL63 are estimated to cause approximately 10 % of all hospitalizations of children for respiratory tract infections (Gerna *et al.*, 2007; Vabret *et al.*, 2008).

A number of animal models exist for the investigation of SARS-CoV, including systems that use mice, guinea pigs, ferrets, cats and rats (Nagata *et al.*, 2007; Roberts *et al.*, 2007; Subbarao & Roberts, 2006; van den Brand *et al.*, 2008). However, no animal models are available for the other, less pathogenic human CoVs 229E, OC43, NL63 and HKU1.

Three supplementary figures are available with the online version of this paper.

Rat coronavirus (RCoV) is a member of the group 2a coronaviruses, like human CoV OC43 and HKU1, and it causes epidemics of respiratory disease in laboratory rat colonies. The two prototype strains of RCoV are sialodacryoadenitis virus (SDAV) and Parker's RCoV (RCoV-P) (Bhatt *et al.*, 1972; Parker *et al.*, 1970). Both strains infect the respiratory tract, and SDAV can also infect the eye, salivary and lacrimal glands. Young rats are especially susceptible to RCoV with the infection occurring in the lower respiratory tract and developing into interstitial pneumonia (Parker *et al.*, 1970; Wojcinski & Percy, 1986).

Although there have been some studies of viral infection in the conducting airways (Johnston, 2005), relatively few have focused on the distal gas exchange unit of the lung, the site of severe clinical infection with SARS-CoV or avian influenza. The epithelium in the gas exchange portions of the lung consists of two main cell types. Alveolar epithelial type I cells are large flat terminally differentiated cells that cover about 95 % of the alveolar surface area and are primarily involved in gas exchange. Cuboidal alveolar type II cells are metabolically active, produce pulmonary surfactant, and transport fluid and sodium to the basolateral surface to keep the alveolar surface suitable for gas exchange (Mason, 2006). They are also self-renewing cells that maintain type II cells and transdifferentiate into type I cells. Both alveolar epithelial cell types participate in the innate immune system, producing interferons and cytokines in response to virus infection (Miura *et al.*, 2007; Wang *et al.*, 2009).

In this study, we sought to identify the cells that RCoV infects in the lower respiratory tract of the natural host. We had shown previously that rat type II cells and type I-like cells could be infected *in vitro* (Miura *et al.*, 2006, 2007). However, we did not know which cells might be infected *in vivo*, the severity of the infection when the virus was inoculated directly into the lung or the nature and extent of the inflammatory response. In general, there is limited information on the pathological pulmonary response to RCoVs *in vivo*.

METHODS

Viruses and cells. SDAV and RCoV-P isolates were obtained from Dr D. Percy (Percy *et al.*, 1991) (University of Guelph, Guelph, Ontario) and propagated in mouse L2P-41.a cells (Gagneten *et al.*, 1996). Virus stocks used for animal inoculation were harvested as supernatants from infected L2P-41.a cultures. The supernatant media were clarified of cell debris by centrifugation and aliquots were stored at –80 °C. Supernatants used for mock (control) inoculation of animals were harvested from uninfected L2P-41.a cell cultures grown under the same conditions and aliquots were also stored at –80 °C. Viral titres of RCoV were determined by plaque assay on L2P-41.a cell cultures as described previously (Miura *et al.*, 2007).

Animals and viral inoculation by intratracheal instillation. Pathogen-free male Fischer 344 rats were obtained from Harlan Laboratories (Indianapolis, IN), whose colonies were negative for SDAV infection by serology. Rats that were inoculated had a weight range of 184–261 g at the time of instillation. The Institutional Animal Care and Use Committee of National Jewish Health approved the animal use protocol. Rats were anaesthetized and sedated by intraperitoneal injection of ketamine (50 mg kg^{-1}), xylazine (5 mg kg^{-1}) and acepromazine (1 mg kg^{-1}). Rats placed in a supine position were inoculated using intratracheal instillation as described previously (Rancourt *et al.*, 2007). Briefly, the oropharynx and larynx were visualized with a fibre optic light and a microspray device that delivers 16–22 μm particles (model IA-1C; Penn-Century) was inserted past the vocal cords and into the trachea; 100 μl of either virus (6×10^5 p.f.u. SDAV per rat) or control medium was aerosolized and delivered into the airway. Two cohorts of rats were infected. Cohort 1 was harvested on days 2, 4, 8 and 12 after instillation and consisted of 4–5 rats per time point. Rat weights were recorded on a daily basis during the infection for Cohort 1. Cohort 2 was harvested at 0.5, 1 and 2 days after instillation with 3–4 rats per time point. At each time point, the left lung was tied-off and then removed. Half of the left lung was flash frozen in liquid nitrogen and stored at −80 °C for virus titration, and the other half of the left lung was incubated in RNAlater (Ambion) for 1 day at 4 °C and then stored at −80 °C. The right lung was lavaged twice with 5 ml buffered salt solution to recover bronchoalveolar lavage fluid (BALF). Cells from the BALF were counted using a haemocytometer and a differential cell count was made from Cytospin slides (Thermo Scientific) stained with Wright's stain (Hemacount; Fisher Scientific). Statistical analysis of cell counts using an unpaired *t*-test with Welch's correction was performed using Prism 4 for Macintosh (GraphPad Software). Cells in the remaining BALF were removed by centrifugation and the BALF was frozen at −80 °C for use in ELISAs. The right lung was fixed and inflated using a 1 % agarose, 1 % paraformaldehyde in buffered salt solution, and then fixed overnight with 4 % PFA (Halbower *et al.*, 1994).

Histology and slide scanning Tissue sections (4 μm) of the right lung were deparaffinized and rehydrated, and then stained with haematoxylin and eosin. To quantify areas with cell infiltrates, whole sections were scanned by ScanScope (Aperio Technologies) at a ×20 magnification. Whole section images (two sections per rat; $n=4$ rats per time point) were viewed and analysed with ImageScope (Aperio), an image viewer software package.

Immunofluorescent antibody (IFA) staining. Viral and cell antigens were detected in deparaffinized and rehydrated lung tissue sections cut at 4 μm. Virus antigen was detected with a mouse monoclonal antibody (mAb) to mouse hepatitis virus nucleocapsid (MHV-N) protein (kindly provided by Dr J. Leibowitz, Texas A&M University, College Station, TX) or with a rabbit polyclonal antibody to MHV-N (anti-MHV-N142). The anti-MHV-N antibodies were detected using an Alexa Fluor 594-conjugated secondary antibody to mouse or rabbit IgG, respectively (Invitrogen). Cell markers for cell identification were: a mouse mAb to T1α for detection of alveolar type I cells (a gift from Dr Mary Williams, Boston University), a mouse mAb to TTF-1 for the detection of alveolar type II cells (clone SPT24; Novocastra, Leica Microsystems), a mouse mAb to rat CD68 (clone ED-1; Chemicon International) for detection of macrophages, a mouse mAb to acetylated tubulin for detection of ciliated airway epithelial cells (Clone 6-11B-1; Sigma), a goat anti-Clara cell secretory protein (CCSP) for detection of Clara cells (a generous gift from Susan Reynolds, National Jewish Health, Denver, CO) and a rabbit polyclonal antibody to rat calcitonin gene-related peptide (CGRP; Sigma) for detection of neuroendocrine cells. The cell marker antibodies bound to the sections were detected using Alexa Fluor 488-conjugated secondary antibodies (Invitrogen). Antigen retrieval was carried out with mAb MHV-N, polyclonal MHV-N142 and anti-CGRP, -CD68 and -TTF-1, and consisted of boiling slides in a microwave pressure cooker (Tender Cooker; Nordic Ware) for 10 min in 0.01 M citrate buffer (pH 6.0) prior to staining with the primary antibody. Sections were mounted in Vectashield Mounting

Medium with DAPI (Vector Laboratories). Sections were visualized by immunofluoresence microscopy using a Zeiss Axioskop2 microscope and AxioVision software package (Zeiss).

Cytokine antibody array. BALF samples from rats inoculated with SDAV or control media were incubated with membranes spotted with antibodies specific for rat cytokines and chemokines (Rat Cytokine Array I; RayBiotech), and the membranes were processed according to the manufacturer's recommendations. The array is designed to detect the following rat proteins: CINC-2, CINC-3, CNTF, fractalkine, GM-CSF, IFN-γ, IL-1α, IL-1β, IL-4, IL-6, IL-10, LIX, leptin, MCP-1, MIP-3α, β-NGF, TIMP-1, TNF-α and VEGF. The membranes (n=3) were exposed to X-ray film and the film was scanned for densitometry analysis using ImageJ (National Institutes of Health). Densitometry data were normalized to internal positive controls on each membrane and graphed as relative units using the Raybio Analysis Tool, a spreadsheet for array analysis.

Cytokine ELISAs. BALF samples from rats inoculated with SDAV or control media were harvested on days 2, 4, 8 and 12 post-inoculation (p.i.) (n=4 per time point). Quantification of CINC-1, MCP-1 and LIX was done by ELISAs from ELISA Tech. The absorbance was read at an optical density of 490 nm, using a MicroQuant microplate reader and analysed with KCjunior Data Analysis Software (Bio-Tek Instruments). Statistical analysis using unpaired t-test with Welch's correction was performed using Prism 4 for Macintosh (GraphPad Software).

Protein assays. Protein concentrations of BALF samples (after cells were pelleted) were measured by the bicinchoninic acid method (Pierce). Protein concentrations in lung homogenates were measured using the Bradford assay (Bio-Rad).

Measurement of SP-A and SP-D in BALF. Polyclonal anti-rat-SP-A or -SP-D rabbit IgG was bound to wells overnight at room temperature (1 μg per well in 0.1 M sodium bicarbonate) in 96-well microtitre plates (Immulon 1 plates, Dynatech Laboratories). The wells were then incubated with blocking buffer [4 % (w/v) solution of non-fat dry milk in PBS with 1 % Triton X-100] for at least 30 min at room temperature. The BALF samples were added, and the ELISA was performed as described previously (Mason *et al.*, 2002). Purified recombinant rat SP-A and SP-D proteins produced in Chinese hamster ovary cells were used as the SP-A and SP-D standards. The standards and antibodies were generous gifts from Dennis Voelker (National Jewish Health, Denver, CO). The absorbance was read at an optical density of 490 nm, recorded with MicroQuant microplate reader and analysed with KCjunior Data Analysis Software (Bio-Tek Instruments).

Quantitative real-time PCR. Half of the rat left lung was preserved with RNAlater (Ambion) and stored at −80 °C. Frozen rat lung pieces were homogenized into 4 M guanidinium isothiocyanate, 0.5 % *N*-laurylsarcosine and 0.1 M β-mercaptoethanol in 25 mM sodium citrate buffer. Total RNA was extracted from the homogenate using Trizol reagent according to the manufacturer's specifications (Invitrogen). The isolated RNA was quantified using a Nanodrop 1000 spectrophotomter (Wilmington, DE) and 1 μg RNA was used to synthesize cDNA using TaqMan reverse transcription reagents (Applied Biosystems) and random hexamer primers. The cDNA reactions were incubated at 25 °C for 10 min, 48 °C for 30 min and 95 °C for 5 min, and then stored at −20 °C. TaqMan PCR (Applied Bioscience) was performed on an ABI Prism 7700 sequence detection system using an IP-10 gene-specific primer/probe set (labelled with FAM) and a GAPDH primer/probe set (labelled with VIC) as an internal control. Q-gene software was used to quantify gene expression based on cycle threshold values normalized to GAPDH expression (Muller *et al.*, 2002).

RESULTS

Intratracheal instillation with SDAV induces weight loss and pulmonary cellular infiltrates

In order to target the RCoV infection directly to the lower respiratory tract, Fischer 344 rats were inoculated with RCoV or control medium by intratracheal instillation using a microspray apparatus. Beginning on day 2 p.i., rats inoculated with SDAV lost weight relative to control rats (Fig. 1a). A preliminary study indicated that instillation of RCoV-P did not produce significant weight loss or pathological changes, and resulted in limited viral replication in the lung (data not shown). Therefore, further studies used only the SDAV strain. SDAV-infected rats continued to lose weight through day 5 p.i. with a mean 7 % body weight loss, followed by weight gain on days 6–12. On days 2 and 4 p.i., the number of cells in BALF increased significantly (Fig. 1b) then decreased to near the initial levels by day 8. Macrophages were markedly elevated on days 2 and 4 p.i. (Fig. 1c). Neutrophils accounted for most of the change in BALF cells from rats on day 2 of the infection, increasing from 6.6 % in control rats to 45 % of the lavage cells in infected rats (Fig. 1d). On day 4 p.i., the number of neutrophils decreased while macrophage numbers increased, causing no net change relative to the number of cells in BALF on day 2. The protein levels in BALF peaked on day 4 (Fig. 1e), indicating an increase in permeability of the alveolar epithelium. Infectious SDAV virus reached titres of 4.3×10^6 p.f.u. (g lung tissue)$^{-1}$ on day 2 and 2.0×10^5 p.f.u. (g lung tissue)$^{-1}$ on day 4 p.i. At later time points, infectious virus was not detected (Supplementary Fig. S1, available in JGV Online).

SDAV causes focal pneumonia in rats

We observed gross pathological changes on the lungs starting on day 2 p.i., with small inflammatory and haemorrhagic lesions. Lung lesions reached a peak on day 4, being larger and present in both lungs. By day 8 p.i., the lesions were smaller and on day 12, no lesions were observed. Whole lung sections stained with haematoxylin and eosin from both SDAV and control rats were examined. Intratracheal inoculation of SDAV into rat lungs resulted in focal pneumonia consisting of cellular infiltrates into the alveolar spaces (Fig. 2a). Other areas of the infected lung (Fig. 2a) were similar to the control lung sections (Fig. 2b). The area of lung with cellular infiltrates reached a peak at day 4 p.i. with an average of 10 % of the area affected by the virus infection (Fig. 2c).

SDAV causes infection in ciliated bronchial epithelial cells, Clara cells and alveolar epithelial type I and type II cells

Viral nucleocapsid antigen was detected in a number of cells types in both the airways and the alveolar areas (Figs 3 and 4). Within the lung and airway, viral antigen could be

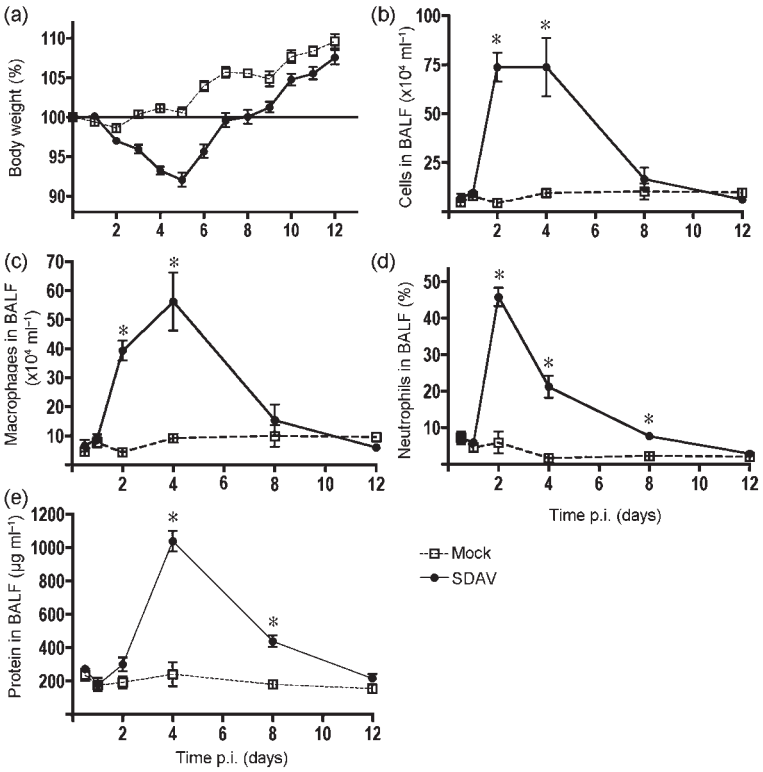

Fig. 1. Changes in body weight and cell and protein levels in BALF after SDAV inoculation. The rats were infected in two cohorts. Cohort 1 was harvested on days 2, 4, 8 and 12 after instillation (n=4–5 rats per time point) and Cohort 2 was harvested at 0.5, 1 and 2 days after instillation (n=3–4 rats per time point). (a) Rat weights were recorded each day and lungs were harvested on days 0.5, 1, 2, 4, 8 and 12. (b, c and d) Cells from BALF were counted on a haemocytometer and scored on cytospin slides. (e) BALF protein levels were determined by bicinchonic acid protein assay. Asterisks indicate statistical significance (P<0.05) between SDAV and control samples.

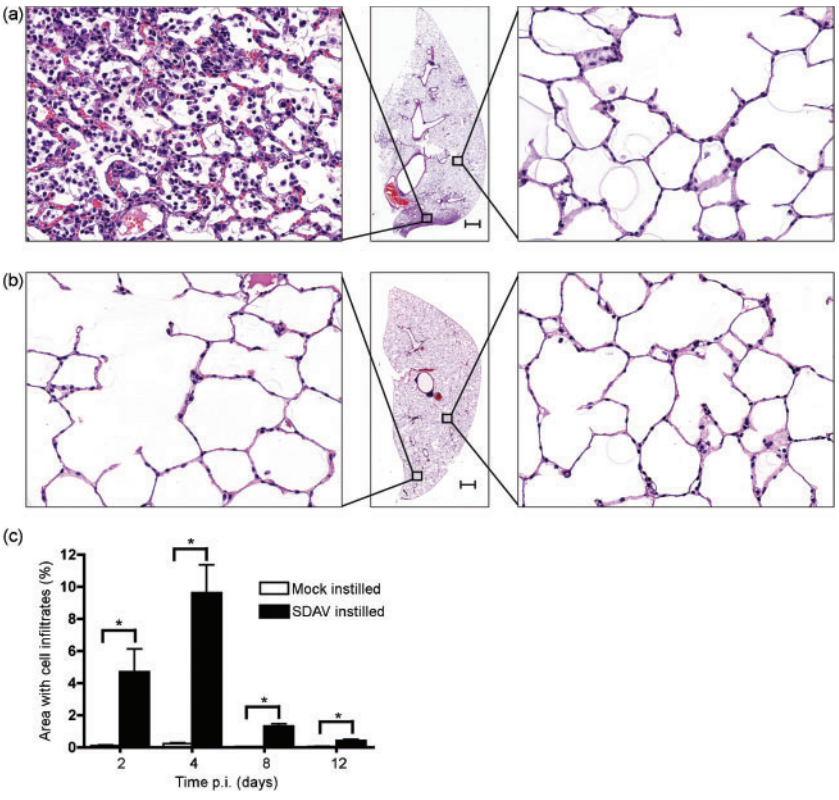

Fig. 2. Lung pathology after SDAV infection. Sections of lung were stained with haematoxylin and eosin. (a) SDAV-instilled rats produced focal pulmonary lesions on day 4. (b) Mock-instilled rats did not have cellular infiltrates in alveoli. Bars in (a) and (b), 1 mm. (c) Whole slide images of haematoxylin and eosin slides were created using an automated scanning system (Aperio Technologies). Regions of the lung sections that had cellular infiltrates were scored by a pathologist. Asterisks indicate statistical significance (P<0.05) between SDAV and control samples. Error bars, SEM.

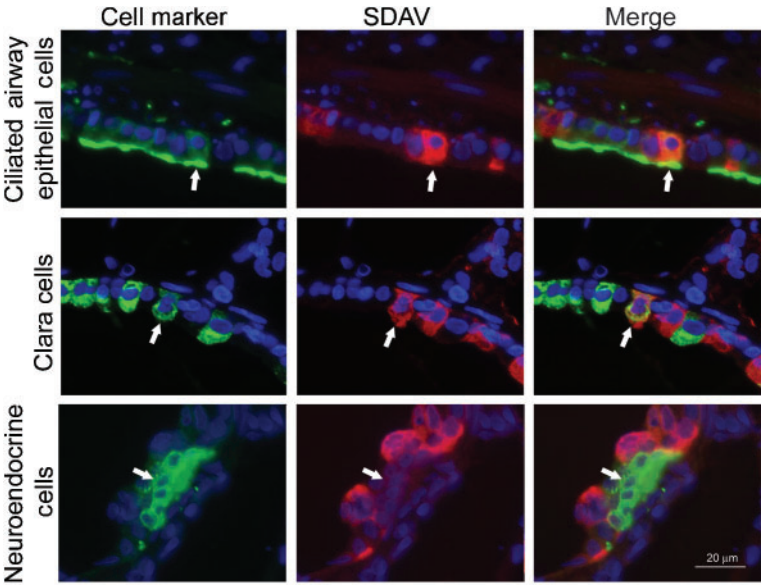

Fig. 3. Identification of the cell types infected in the conducting airways. Rat lung paraffin sections were stained for cell markers (Alexa 488; green secondary antibody), SDAV (Alexa 594; red secondary antibody) and nuclei (DAPI; blue). Markers for ciliated cells (acetylated tubulin antibody), Clara cells (CCSP antibody) and neuroendocrine cells (CGRP antibody) were used to identify cell types. SDAV was localized with an anti-MHV rabbit polyclonal antibody. Viral antigen for SDAV was localized to ciliated cells and Clara cells, but not neuroendocrine cells. Arrows indicate a cell identified by the marker antibody. Bar, 20 μm.

detected within cells as early as 12 h p.i. Cell markers were used to identify infected cell types (Supplementary Fig. S2, available in JGV Online, shows additional images of uninfected controls). However, as the infection proceeded, identification of infected cells became more difficult due to loss of marker expression in the infected cells. Within the bronchial airway, both ciliated cells and Clara cells were infected (Fig. 3). However, another cell population lining the airway, neuroendocrine cells, were not infected (Fig. 3). The predominant cells infected in the alveolar walls were type I epithelial cells (Fig. 4). Within infected areas of the lung, type I cells had thickened cell walls and showed abundant viral antigen staining (Supplementary Fig. S3, available in JGV Online). A few of the type II cells within the affected lung areas were also infected by SDAV (Fig. 4). Viral antigen was not detected in alveolar macrophages (Fig. 4).

Rat lung infection by SDAV induces expression of cytokines LIX, MCP-1, CINC-1, IP-10 and surfactant protein SP-D

The influx of inflammatory cells present in BALF suggested that SDAV infection induced secretion of cytokines and chemokines. To identify cytokines and chemokines induced by the infection, BALF from day 4 p.i. was assayed for the presence of cytokines using an antibody-based cytokine array (Fig. 5). We were particularly interested in

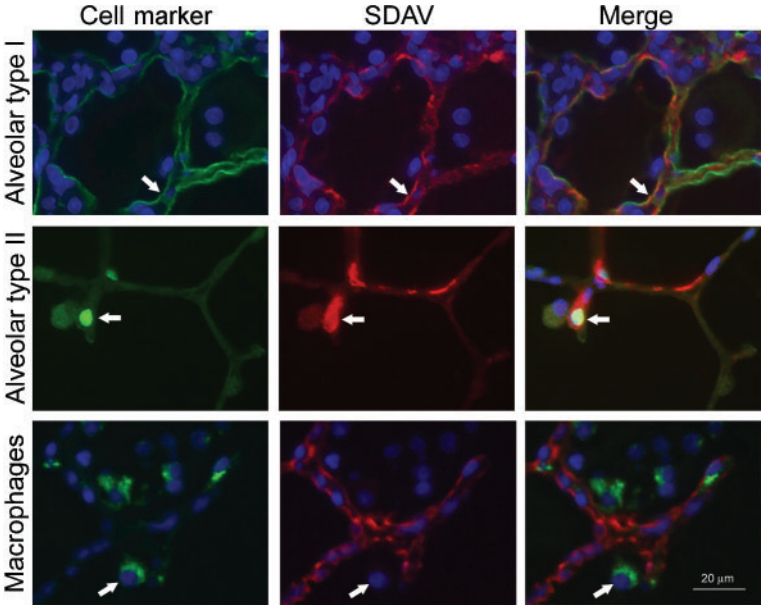

Fig. 4. Identification of the cell types infected in the alveolar region. Rat lung paraffin sections were stained for cell markers (Alexa 488; green secondary antibody), SDAV (Alexa 594; red secondary antibody) and nuclei (DAPI; blue). Markers for alveolar epithelial type I cells (T1-α antibody), alveolar epithelial type II cells (TTF-1) and macrophages (rat CD68) were used to localize cells. SDAV was localized with an anti-MHV rabbit polyclonal antibody. Arrows indicate a cell identified by the marker antibody. Bar, 20 μm.

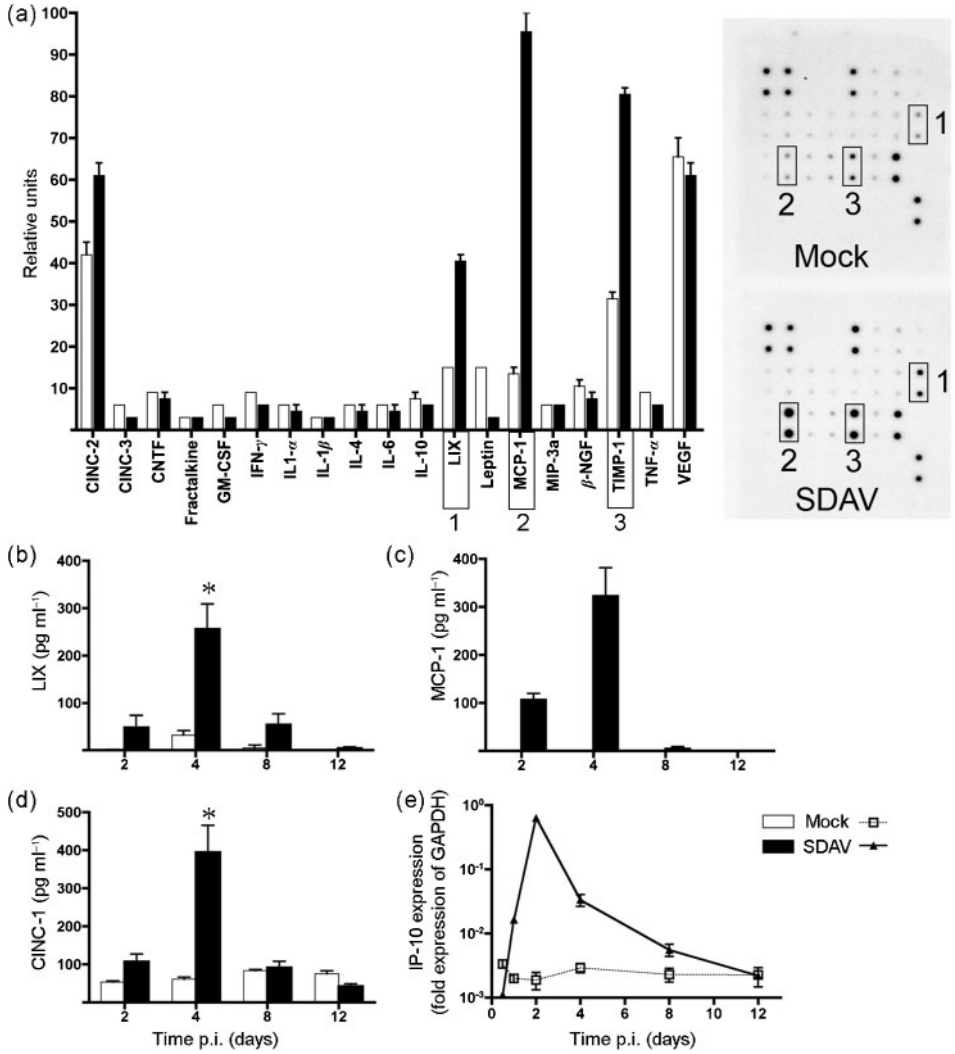

Fig. 5. Cytokine expression by SDAV-infected rats. (a) BALF from SDAV- and mock-infected rats was analysed for cytokine and chemokine secretion using antibody arrays. Densitometry data were normalized to internal positive controls on each membrane ($n=3$) and graphed as relative units. Scans of autoradiographs for each membrane are shown to the right of the graph with relevant duplicate spots boxed with numbers corresponding to cytokines on the graph. (b–d) Cytokine levels for LIX, MCP-1 and CINC-1 were assayed in BALF using ELISA assays. All of the mock-instilled values for cytokine MCP-1 were below the level of detection. Asterisks indicate a statistically significant difference ($P<0.05$) compared with control samples. (e) Real-time quantitative PCR analysis of cytokine IP-10 expression. Error bars, SEM.

neutrophil chemotactants LIX (CXCL5), CINC-1 and CINC-2 and the macrophage chemokine MCP-1 (CCL2). Of the 19 rat cytokines and proteins detected by the array, LIX, MCP-1 and TIMP-1 increased by at least twofold in the samples from the SDAV rats compared with control rats. CINC-2 levels also increased on the array, but to a lesser extent (Fig. 5a). Increased levels of LIX and MCP-1 were confirmed using ELISA assays, whereas TIMP-1, a metalloproteinase inhibitor, was not investigated further. Secretion of LIX and MCP-1 peaked on day 4 p.i. and returned to baseline levels by day 8 (Fig. 5b and c). The levels of CINC-1, a CXC chemokine and neutrophil chemoattractant, also increased in BALF samples, peaking at day 4 p.i. (Fig. 5d). In addition, RNA expression levels for IP-10 (CXCL10), a monocyte and lymphocyte chemoattractant, were monitored using real-time quantitative PCR. IP-10 expression peaked at day 2 p.i. and then returned to control levels by day 12 (Fig. 5e).

Two important proteins of the innate immune system in the gas exchange portion of the lung are surfactant proteins A and D (Haagsman *et al.*, 2008; Pastva *et al.*, 2007), both of which have been reported to be important in controlling viral infections (Doss *et al.*, 2009; Leth-Larsen *et al.*, 2007). BALF samples from SDAV and control rats were assayed for surfactant proteins SP-A and SP-D using ELISA (Fig. 6).

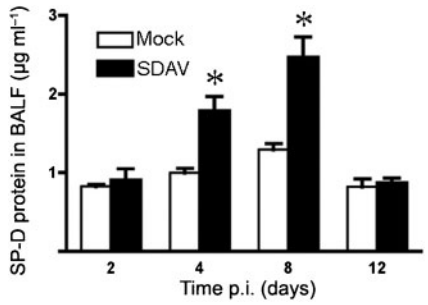

Fig. 6. SP-D expression by SDAV-infected rats. BALF was collected from rat lungs at the indicated times after intratracheal inoculation. SP-D expression was measured by ELISA. Results are means ± SEM of four rats per time point.

In SDAV-infected rats, SP-D levels were significantly higher on days 4 and 8 p.i., but not at earlier or later times. SP-A levels in BALF did not change in response to the SDAV infection (not shown).

DISCUSSION

Respiratory viral infections cause a significant amount of global morbidity and mortality (Kesson, 2007; Nichols *et al.*, 2008). However, the types of cells infected within the respiratory tract can vary depending on the virus. Therefore, it is important to identify the cells that are the major target of infection in order to develop an optimal *in vitro* system for studying the virus. A previous study of SDAV infections in the rat lower respiratory tract observed that there was viral antigen in bronchial epithelial cells, but the infected cell types were not identified (Wojcinski & Percy, 1986). We demonstrated that intratracheal inoculation of SDAV into F344 rats results in viral infection of specific cell types in the bronchial airway and the lung parenchyma. Within the airway, both Clara cells and ciliated epithelial cells were infected, but neuroendocrine cells were not. In the lung parenchyma, the main target of the infection was alveolar epithelial type I cells. Type II cells were occasionally infected whereas alveolar macrophages were not infected. In comparison, a number of studies have identified cells of the human respiratory tract that are infected by SARS-CoV. Initial reports based on the cytopathology of biopsy and autopsy samples indicated that type I and type II alveolar epithelial cells were infected (Franks *et al.*, 2003; Nicholls *et al.*, 2003; Peiris *et al.*, 2003). This was later confirmed by localization of SARS-CoV antigen in type II and type I cells and bronchiolar epithelial cells (Nicholls *et al.*, 2006; Shieh *et al.*, 2005). Infection of alveolar macrophages seemed to vary with the patient, with positive virus staining of CD68 cells in some individuals, but not others (Nicholls *et al.*, 2006; Shieh *et al.*, 2005; To *et al.*, 2004). Using primary cell culture systems, SARS-CoV has been shown to replicate in type II cells, but not type I-like cells and alveolar macrophages *in vitro* (Mossel *et al.*, 2008). Human ciliated airway epithelial cell cultures and lung stem cells that express CCSP can also support growth of SARS-CoV (Ling *et al.*, 2006; Sims *et al.*, 2005). Therefore, the specific respiratory tract cell types targeted by both SDAV following intratracheal inoculation of rats and by SARS-CoV infection of humans are very similar; both infect alveolar type I and type II cells in the lung parenchyma and epithelial cells in the bronchial airway.

Surfactant proteins SP-A and SP-D are produced by type II cells and are capable of binding to and inactivating pathogens, including viruses (Crouch, 2000; Haagsman, 1998). The changes in surfactant protein expression (mRNA or protein) during infection appear to depend on the virus. The protein level of SP-D rose in response to influenza virus infection of mice (Reading *et al.*, 1997). However, protein levels of SP-A decreased in response to respiratory syncytial virus infection (Alcorn *et al.*, 2005). Following infection by parainfluenza virus type 3, the SP-A mRNA levels increased, but the protein levels of SP-A were not altered (Grubor *et al.*, 2004). In our study, SP-D protein expression increased in response to the viral infection compared with mock-instilled controls, but SP-A did not, suggesting an important role for SP-D as part of the innate immune response to the virus infection.

The levels of cytokines produced during viral infections can vary greatly depending on the virus isolate and the host species. The significant morbidity and mortality caused by SARS-CoV are thought to be largely due to dysregulated release of cytokines, in the form of a 'cytokine storm' (Huang *et al.*, 2005). Patients with SARS showed marked elevation of inflammatory cytokines IFN-γ, IL-1, IL-6 and IL-12, along with chemokines IL-8, MCP-1 and IP-10 in plasma (Wong *et al.*, 2004). In our study, the levels of inflammatory cytokines IL-1α, IL-1β, TNF-α, IFN-γ and IL-6 in BALF did not increase significantly following infection, but chemokines that were upregulated following SDAV infection were similar to those found in a SARS-CoV infection. Levels of chemokines LIX and MCP-1 had the greatest increase of all of the chemokines on the antibody array. In addition, CINC-1 (protein) and IP-10 (RNA) also increased significantly, as determined by ELISA and real-time PCR analysis, respectively. Although chemokines can have multiple functions, CINC-1 and LIX from the IL-8 family have a role in neutrophil chemoattraction, whereas MCP-1 and IP-10 are chemotactic for monocytes and macrophages. The increased levels of these chemokines following infection by SDAV likely leads to the large increase in neutrophils and macrophages in the BALF. Much of the observed cytokine production is likely due to infection of the type I epithelial cells. In a primary rat alveolar type I-like cell culture system, we showed that the main cytokines released at 24 h after inoculation with SDAV were CXC chemokines, CINC-2, CINC-3 and LIX (Miura *et al.*, 2007). The chemokine signal originates mainly from uninfected cells using an IL-1 pathway. Identification of type I cells as the primary target of infection within the alveolus is confirmation of the

importance of the type I-like primary cell system for analysis of the innate immune response to epithelial cell infection (Miura *et al.*, 2007). It also confirms the importance of CXC chemokine expression following SDAV infection for neutrophil and macrophage influx in a coronaviral respiratory virus system.

The five CoVs known to infect humans are all pathogens of the respiratory tract. Although several animal model systems have been used for investigation of SARS-CoV infections (Subbarao & Roberts, 2006), good animal models are not available for the other four human CoVs (229E, OC43, NL63 and HKU1). Although these four human CoVs typically infect the upper respiratory tract, they are also known to infect the lower respiratory tract, especially in infants, elderly and immunocompromised patients (Gerna *et al.*, 2006; Kahn, 2006). However, the MHV-1 strain of murine CoV is being used as an animal model for respiratory CoV infection in A/J mice (De Albuquerque *et al.*, 2006; Khanolkar *et al.*, 2009). The MHV-1 model is quite different from RCoV infection of adult rats. In A/J mice, MHV-1 infection is lethal, whereas SDAV infection in rats is not. MHV-1 predominantly infects macrophages, whereas SDAV primarily infects epithelial cells, and therefore the pathogenesis of these two viral infections is likely to be very different. RCoV infection in its natural host can serve as an animal model system for human CoV pathogens that cause non-fatal respiratory diseases. The other major advantage of the rat model is that alveolar type II cells and type I-like cells can be readily isolated for *in vitro* studies, and parallel studies in mice are much more challenging. The tropism of RCoV for alveolar epithelial cells makes it an ideal model in which to study the mechanisms by which alveolar epithelial cells influence antiviral immune responses in the lung. Together, the rat *in vitro* and *in vivo* systems can be used for further investigations of viral pathogenesis, CXC chemokine expression and neutrophil and macrophage migration into the lung, and can provide a platform for antiviral drug studies.

ACKNOWLEDGEMENTS

We thank Dr Dennis Voelker and Mandy Evans for the standards and polyclonal antibodies used in the SP-A and SP-D ELISAs, and Dr Susan Reynolds for generously providing antibodies. We appreciate Dr Raymond Rancourt's instruction on the rat intratracheal instillation method and Dr Donna Bratton's helpful discussions. We also thank Dr Mary Williams for the generous of gift of the T1α antibody. We appreciate the assistance with manuscript preparation provided by Margaret Willett and Teneke M. Warren. This research was funded by National Institutes of Health program project grant #5P01AI059576. T. M. is supported by grant P20RR015587 from NCRR/NIH.

REFERENCES

Alcorn, J. L., Stark, J. M., Chiappetta, C. L., Jenkins, G. & Colasurdo, G. N. (2005). Effects of RSV infection on pulmonary surfactant protein SP-A in cultured human type II cells: contrasting consequences on SP-A mRNA and protein. *Am J Physiol Lung Cell Mol Physiol* **289**, L1113–L1122.

Bhatt, P. N., Percy, D. H. & Jonas, A. M. (1972). Characterization of the virus of sialodacryoadenitis of rats: a member of the coronavirus group. *J Infect Dis* **126**, 123–130.

Crouch, E. C. (2000). Surfactant protein-D and pulmonary host defense. *Respir Res* **1**, 93–108.

De Albuquerque, N., Baig, E., Ma, X., Zhang, J., He, W., Rowe, A., Habal, M., Liu, M., Shalev, I. & other authors (2006). Murine hepatitis virus strain 1 produces a clinically relevant model of severe acute respiratory syndrome in A/J mice. *J Virol* **80**, 10382–10394.

Doss, M., White, M. R., Tecle, T., Gantz, D., Crouch, E. C., Jung, G., Ruchala, P., Waring, A. J., Lehrer, R. I. & Hartshorn, K. L. (2009). Interactions of alpha-, beta-, and theta-defensins with influenza A virus and surfactant protein D. *J Immunol* **182**, 7878–7887.

Fouchier, R. A., Kuiken, T., Schutten, M., van Amerongen, G., van Doornum, G. J., van den Hoogen, B. G., Peiris, M., Lim, W., Stohr, K. & Osterhaus, A. D. (2003). Aetiology: Koch's postulates fulfilled for SARS virus. *Nature* **423**, 240.

Franks, T. J., Chong, P. Y., Chui, P., Galvin, J. R., Lourens, R. M., Reid, A. H., Selbs, E., McEvoy, C. P., Hayden, C. D. & other authors (2003). Lung pathology of severe acute respiratory syndrome (SARS): a study of 8 autopsy cases from Singapore. *Hum Pathol* **34**, 743–748.

Gagneten, S., Scanga, C. A., Dveksler, G. S., Beauchemin, N., Percy, D. & Holmes, K. V. (1996). Attachment glycoproteins and receptor specificity of rat coronaviruses. *Lab Anim Sci* **46**, 159–166.

Gerna, G., Campanini, G., Rovida, F., Percivalle, E., Sarasini, A., Marchi, A. & Baldanti, F. (2006). Genetic variability of human coronavirus OC43-, 229E-, and NL63-like strains and their association with lower respiratory tract infections of hospitalized infants and immunocompromised patients. *J Med Virol* **78**, 938–949.

Gerna, G., Percivalle, E., Sarasini, A., Campanini, G., Piralla, A., Rovida, F., Genini, E., Marchi, A. & Baldanti, F. (2007). Human respiratory coronavirus HKU1 versus other coronavirus infections in Italian hospitalised patients. *J Clin Virol* **38**, 244–250.

Grubor, B., Gallup, J. M., Meyerholz, D. K., Crouch, E. C., Evans, R. B., Brogden, K. A., Lehmkuhl, H. D. & Ackermann, M. R. (2004). Enhanced surfactant protein and defensin mRNA levels and reduced viral replication during parainfluenza virus type 3 pneumonia in neonatal lambs. *Clin Diagn Lab Immunol* **11**, 599–607.

Haagsman, H. P. (1998). Interactions of surfactant protein A with pathogens. *Biochim Biophys Acta* **1408**, 264–277.

Haagsman, H. P., Hogenkamp, A., van Eijk, M. & Veldhuizen, E. J. (2008). Surfactant collectins and innate immunity. *Neonatology* **93**, 288–294.

Halbower, A. C., Mason, R. J., Abman, S. H. & Tuder, R. M. (1994). Agarose infiltration improves morphology of cryostat sections of lung. *Lab Invest* **71**, 149–153.

Huang, K. J., Su, I. J., Theron, M., Wu, Y. C., Lai, S. K., Liu, C. C. & Lei, H. Y. (2005). An interferon-gamma-related cytokine storm in SARS patients. *J Med Virol* **75**, 185–194.

Johnston, S. L. (2005). Overview of virus-induced airway disease. *Proc Am Thorac Soc* **2**, 150–156.

Kahn, J. S. & McIntosh, K. (2005). History and recent advances in coronavirus discovery. *Pediatr Infect Dis J* **24**, S223–S227.

Kahn, J. S. (2006). The widening scope of coronaviruses. *Curr Opin Pediatr* **18**, 42–47.

Kesson, A. M. (2007). Respiratory virus infections. *Paediatr Respir Rev* **8**, 240–248.

Khanolkar, A., Hartwig, S. M., Haag, B. A., Meyerholz, D. K., Harty, J. T. & Varga, S. M. (2009). Toll-like receptor 4 deficiency increases disease and mortality after mouse hepatitis virus type 1 infection of susceptible C3H mice. *J Virol* **83**, 8946–8956.

Leth-Larsen, R., Zhong, F., Chow, V. T., Holmskov, U. & Lu, J. (2007). The SARS coronavirus spike glycoprotein is selectively recognized by lung surfactant protein D and activates macrophages. *Immunobiology* **212**, 201–211.

Ling, T. Y., Kuo, M. D., Li, C. L., Yu, A. L., Huang, Y. H., Wu, T. J., Lin, Y. C., Chen, S. H. & Yu, J. (2006). Identification of pulmonary Oct-4$^+$ stem/progenitor cells and demonstration of their susceptibility to SARS coronavirus (SARS-CoV) infection in vitro. *Proc Natl Acad Sci U S A* **103**, 9530–9535.

Mason, R. J. (2006). Biology of alveolar type II cells. *Respirology* **11** (Suppl.), S12–S15.

Mason, R. J., Lewis, M. C., Edeen, K. E., McCormick-Shannon, K., Nielsen, L. D. & Shannon, J. M. (2002). Maintenance of surfactant protein A and D secretion by rat alveolar type II cells in vitro. *Am J Physiol Lung Cell Mol Physiol* **282**, L249–L258.

Miura, T. A., Wang, J., Mason, R. J. & Holmes, K. V. (2006). Rat coronavirus infection of primary rat alveolar epithelial cells. *Adv Exp Med Biol* **581**, 351–356.

Miura, T. A., Wang, J., Holmes, K. V. & Mason, R. J. (2007). Rat coronaviruses infect rat alveolar type I epithelial cells and induce expression of CXC chemokines. *Virology* **369**, 288–298.

Mossel, E. C., Wang, J., Jeffers, S., Edeen, K. E., Wang, S., Cosgrove, G. P., Funk, C. J., Manzer, R., Miura, T. A. & other authors (2008). SARS-CoV replicates in primary human alveolar type II cell cultures but not in type I-like cells. *Virology* **372**, 127–135.

Muller, P. Y., Janovjak, H., Miserez, A. R. & Dobbie, Z. (2002). Processing of gene expression data generated by quantitative real-time RT-PCR. *Biotechniques* **32**, 1372–1379.

Nagata, N., Iwata, N., Hasegawa, H., Fukushi, S., Yokoyama, M., Harashima, A., Sato, Y., Saijo, M., Morikawa, S. & Sata, T. (2007). Participation of both host and virus factors in induction of severe acute respiratory syndrome (SARS) in F344 rats infected with SARS coronavirus. *J Virol* **81**, 1848–1857.

Nicholls, J. M., Poon, L. L., Lee, K. C., Ng, W. F., Lai, S. T., Leung, C. Y., Chu, C. M., Hui, P. K., Mak, K. L. & other authors (2003). Lung pathology of fatal severe acute respiratory syndrome. *Lancet* **361**, 1773–1778.

Nicholls, J. M., Butany, J., Poon, L. L., Chan, K. H., Beh, S. L., Poutanen, S., Peiris, J. S. & Wong, M. (2006). Time course and cellular localization of SARS-CoV nucleoprotein and RNA in lungs from fatal cases of SARS. *PLoS Med* **3**, e27.

Nichols, W. G., Peck Campbell, A. J. & Boeckh, M. (2008). Respiratory viruses other than influenza virus: impact and therapeutic advances. *Clin Microbiol Rev* **21**, 274–290.

Parker, J. C., Cross, S. S. & Rowe, W. P. (1970). Rat coronavirus (RCV): a prevalent, naturally occurring pneumotropic virus of rats. *Arch Gesamte Virusforsch* **31**, 293–302.

Pastva, A. M., Wright, J. R. & Williams, K. L. (2007). Immunomodulatory roles of surfactant proteins A and D: implications in lung disease. *Proc Am Thorac Soc* **4**, 252–257.

Peiris, J. S., Lai, S. T., Poon, L. L., Guan, Y., Yam, L. Y., Lim, W., Nicholls, J., Yee, W. K., Yan, W. W. & other authors (2003). Coronavirus as a possible cause of severe acute respiratory syndrome. *Lancet* **361**, 1319–1325.

Percy, D. H., Williams, K. L. & Paturzo, F. X. (1991). A comparison of the sensitivity and specificity of sialodacryoadenitis virus, Parker's rat coronavirus, and mouse hepatitis virus-infected cells as a source of antigen for the detection of antibody to rat coronaviruses. *Arch Virol* **119**, 175–180.

Rancourt, R. C., Lee, R. L., O'Neill, H., Accurso, F. J. & White, C. W. (2007). Reduced thioredoxin increases proinflammatory cytokines and neutrophil influx in rat airways: modulation by airway mucus. *Free Radic Biol Med* **42**, 1441–1453.

Reading, P. C., Morey, L. S., Crouch, E. C. & Anders, E. M. (1997). Collectin-mediated antiviral host defense of the lung: evidence from influenza virus infection of mice. *J Virol* **71**, 8204–8212.

Roberts, A., Deming, D., Paddock, C. D., Cheng, A., Yount, B., Vogel, L., Herman, B. D., Sheahan, T., Heise, M. & other authors (2007). A mouse-adapted SARS-coronavirus causes disease and mortality in BALB/c mice. *PLoS Pathog* **3**, e5.

Shieh, W. J., Hsiao, C. H., Paddock, C. D., Guarner, J., Goldsmith, C. S., Tatti, K., Packard, M., Mueller, L., Wu, M. Z. & other authors (2005). Immunohistochemical, in situ hybridization, and ultrastructural localization of SARS-associated coronavirus in lung of a fatal case of severe acute respiratory syndrome in Taiwan. *Hum Pathol* **36**, 303–309.

Sims, A. C., Baric, R. S., Yount, B., Burkett, S. E., Collins, P. L. & Pickles, R. J. (2005). Severe acute respiratory syndrome coronavirus infection of human ciliated airway epithelia: role of ciliated cells in viral spread in the conducting airways of the lungs. *J Virol* **79**, 15511–15524.

Subbarao, K. & Roberts, A. (2006). Is there an ideal animal model for SARS? *Trends Microbiol* **14**, 299–303.

To, K. F., Tong, J. H., Chan, P. K., Au, F. W., Chim, S. S., Chan, K. C., Cheung, J. L., Liu, E. Y., Tse, G. M. & other authors (2004). Tissue and cellular tropism of the coronavirus associated with severe acute respiratory syndrome: an in-situ hybridization study of fatal cases. *J Pathol* **202**, 157–163.

Vabret, A., Dina, J., Gouarin, S., Petitjean, J., Tripey, V., Brouard, J. & Freymuth, F. (2008). Human (non-severe acute respiratory syndrome) coronavirus infections in hospitalised children in France. *J Paediatr Child Health* **44**, 176–181.

van den Brand, J. M., Haagmans, B. L., Leijten, L., van Riel, D., Martina, B. E., Osterhaus, A. D. & Kuiken, T. (2008). Pathology of experimental SARS coronavirus infection in cats and ferrets. *Vet Pathol* **45**, 551–562.

van der Hoek, L., Pyrc, K., Jebbink, M. F., Vermeulen-Oost, W., Berkhout, R. J., Wolthers, K. C., Wertheim-van Dillen, P. M., Kaandorp, J., Spaargaren, J. & Berkhout, B. (2004). Identification of a new human coronavirus. *Nat Med* **10**, 368–373.

Wang, J., Oberley-Deegan, R., Wang, S., Nikrad, M., Funk, C. J., Hartshorn, K. L. & Mason, R. J. (2009). Differentiated human alveolar type II cells secrete antiviral IL-29 (IFN-λ1) in response to influenza A infection. *J Immunol* **182**, 1296–1304.

Weiss, S. R. & Navas-Martin, S. (2005). Coronavirus pathogenesis and the emerging pathogen severe acute respiratory syndrome coronavirus. *Microbiol Mol Biol Rev* **69**, 635–664.

WHO (2004). *The World Health Report 2004: Changing History*. World Health Organization.

Wojcinski, Z. W. & Percy, D. H. (1986). Sialodacryoadenitis virus-associated lesions in the lower respiratory tract of rats. *Vet Pathol* **23**, 278–286.

Wong, C. K., Lam, C. W., Wu, A. K., Ip, W. K., Lee, N. L., Chan, I. H., Lit, L. C., Hui, D. S., Chan, M. H. & other authors (2004). Plasma inflammatory cytokines and chemokines in severe acute respiratory syndrome. *Clin Exp Immunol* **136**, 95–103.

Woo, P. C., Lau, S. K., Chu, C. M., Chan, K. H., Tsoi, H. W., Huang, Y., Wong, B. H., Poon, R. W., Cai, J. J. & other authors (2005). Characterization and complete genome sequence of a novel coronavirus, coronavirus HKU1, from patients with pneumonia. *J Virol* **79**, 884–895.